

# THE DECAMETER AND METER WAVE RADIOTELESCOPES IN INDIA AND MAURITIUS

CH. V. SASTRY

*Indian Institute of Astrophysics, Koramangala, Bangalore 560034, India*

(Received 2 January, 1994)

**Abstract.** The Indian Institute of Astrophysics and the Raman Research Institute in a joint collaboration program operate the Gauribidanur radio observatory. Details of the various radiotelescopes available at the observatory are given. A brief account of the results obtained is also presented. A description of the low frequency synthesis radio telescope constructed on the island of Mauritius is also given.

## 1. Introduction

Observations of the radio bursts from the Sun with high temporal and frequency resolution were started using small and medium sized antenna arrays at decameter wavelengths at the Astrophysical Observatory, Kodaikanal, India during late sixties and many interesting results were obtained (Sastry, 1972, 1973). At the same time plans were also made to build a large decameter wave radiotelescope, near Madras. The Astrophysical Observatory became Indian Institute of Astrophysics and was shifted to Bangalore, Karnataka during early seventies. It was then decided to build the large decameter wave radio telescope at Gauribidanur near Bangalore since the Raman Research Institute also joined the project. The construction of this telescope was completed during early eighties and it is being used for various types of solar, galactic and extragalactic observations. The detection of faint ionized hydrogen (H II) regions was one of the major objectives of the study of galactic radio emission. Many H II regions were detected and their temperature and density distributions were studied. It soon became clear that a low frequency radiotelescope which could study the center of the galaxy and other interesting regions in the southern sky would produce exciting new results. A meter wave radiotelescope is therefore built on the island of Mauritius in collaboration with the Raman Research Institute and the University of Mauritius, for studies of the regions around the galactic center and the southern galactic plane.

The decameter wave radio telescope is also used for mapping the continuum emission from the undisturbed Sun in addition to observations on solar radio bursts. It became obvious that maps at several low radio frequencies are necessary for a better understanding of the processes underlying the emission and propagation of the radiation in the outer corona. At present a radioheliograph is being built at the Gauribidanur radio observatory for observations in the frequency range 35 to 150 MHz.

*Space Science Reviews* 72: 629–654, 1995.

© 1995 Kluwer Academic Publishers. Printed in Belgium.

In what follows the technical features of these telescopes are given and the results obtained are briefly discussed.

## 2. The Gauribidanur Radio Observatory

The Indian Institute of Astrophysics and the Raman Research Institute in a joint collaboration program operate this observatory located at Gauribidanur (Lat.:  $13^{\circ}36'12''$  N and Long.:  $77^{\circ}26'07''$  E) about 100 km from Bangalore, India. The facilities at this observatory are presented below.

### 2.1. DECAMETER WAVE RADIOTELESCOPE

The main facility at the observatory is the Decameter Wave Radiotelescope (GBDRT), operating at 34.5 MHz, is essentially a meridian transit instrument although a limited tracking capability is available. The telescope consists of 1000 dipoles arranged in the form of the letter 'T'. A schematic of the dipole used in the array is shown in Figure 1. Its usable bandwidth is 10 MHz centered at 32 MHz. The outputs of four such dipoles along the east–west direction are combined in a branched feeder system using open wire transmission lines, transformers and a balun to form the basic array element as shown in Figure 2. Such basic elements, numbering 250 are arranged to form a 1.38 km long E–W array along the east–west direction and a 0.45 km long S array extending southwards from the center of the E–W array as shown in Figure 3.

The E–W array consists of ten groups of 16 basic elements each. In each one of these groups, the 16 basic elements are arranged in the form of  $4 \times 4$  matrix. The outputs of the basic elements are combined as shown in Figure 4 to produce a group output. Five group outputs available from each of the east and west arms, are combined separately and the amplified outputs of the east and west arms are brought to the receiver room (Figure 5).

The S array consists of 90 basic elements arranged along the N–S direction. The output of each element is amplified using a FET preamplifier. These amplified outputs are then combined together in a Christmas tree fashion using diode phase shifters, power combiners and amplifiers at appropriate stages as shown in Figure 6. This final output is brought to the receiver room.

The beams of both the arrays can be tilted in the N–S direction with the help of the diode phase shifters used in the feeder system. A special purpose control system is used to generate appropriate control signals for these phase shifters. When the outputs of the E–W and S arms are correlated in phase a pencil beam of half power width  $26' \times 38'$   $\sec(z)$  is obtained where  $z$  is the zenith angle. This correlation beam can be pointed to any direction along the meridian within a declination range of  $+45^{\circ}$  to  $+75^{\circ}$  in steps of 12 arc min. The time required to change the beam from one position to another is about 10 ms and the number of positions through which

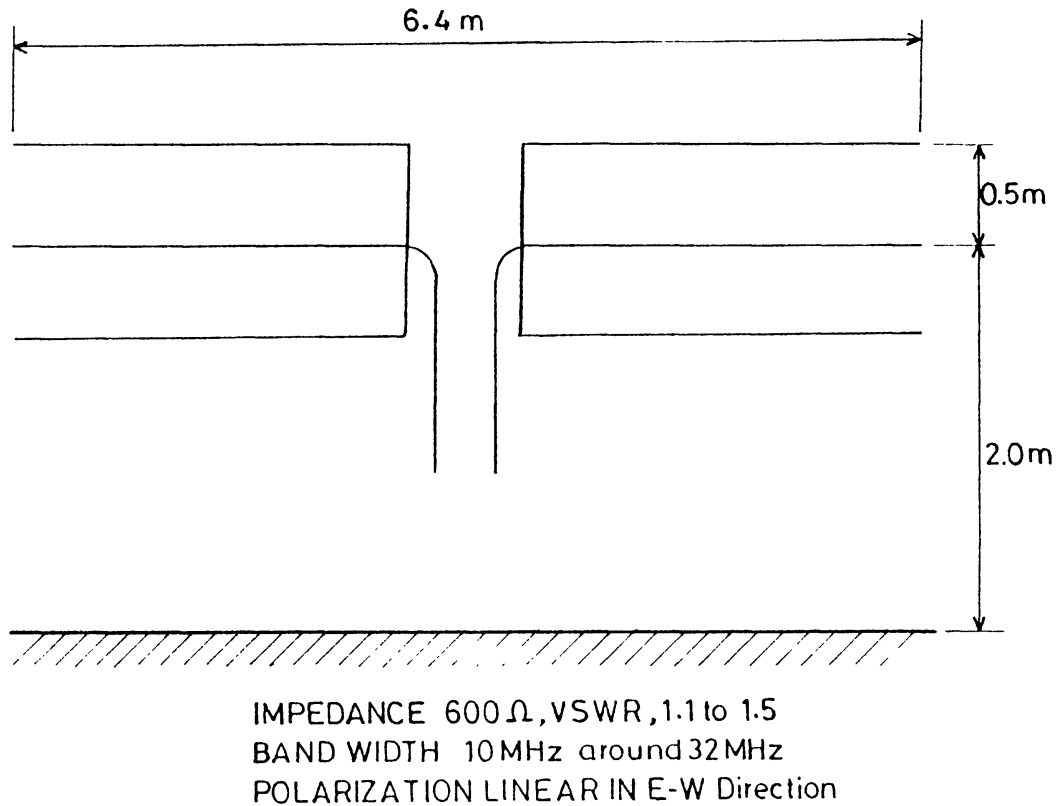


Fig. 1. A schematic of the dipole used in the Gauribidanur decameter radiotelescope (GBDRT).

the beam can be cycled can be varied from one to sixteen. The ideal beam patterns in the E–W and N–S directions corresponding to the inphase correlation are close to sinc functions. Because the beamwidth in the E–W direction is 26 arc min, a point source can be observed for only about  $2 s(\delta)$  min where  $\delta$  is the declination of the source (Deshpande *et al.*, 1989).

The point source sensitivity of this telescope for continuum observations is confusion limited due to the limited angular resolution. However, for observations of weak pulsar signals, low-frequency recombination lines, and interplanetary scintillations the sensitivity attainable with the meridian transit telescope is not adequate. A tracking system is therefore incorporated in the E–W array to enable observations over long periods with the maximum possible collecting area of the entire ‘T’. Using this system the E–W beam can be tilted in hour angle within  $\pm 7.5^\circ$  from the meridian. This is achieved by introducing appropriate phase gradients across the E–W array using diode phase shifters and a special purpose digital control system. It is thus possible to observe a source for  $42 s(\delta)$  min.

In order to increase the resolving power in declination and also the total collecting area an array of 64 Yagis is placed at a distance of 0.45 km in the northerly direction from the center of the E–W arm of the ‘T’ as shown in Figure 3. The beam of this array can be pointed anywhere within  $\pm 50^\circ$  of the zenith on the meridian.

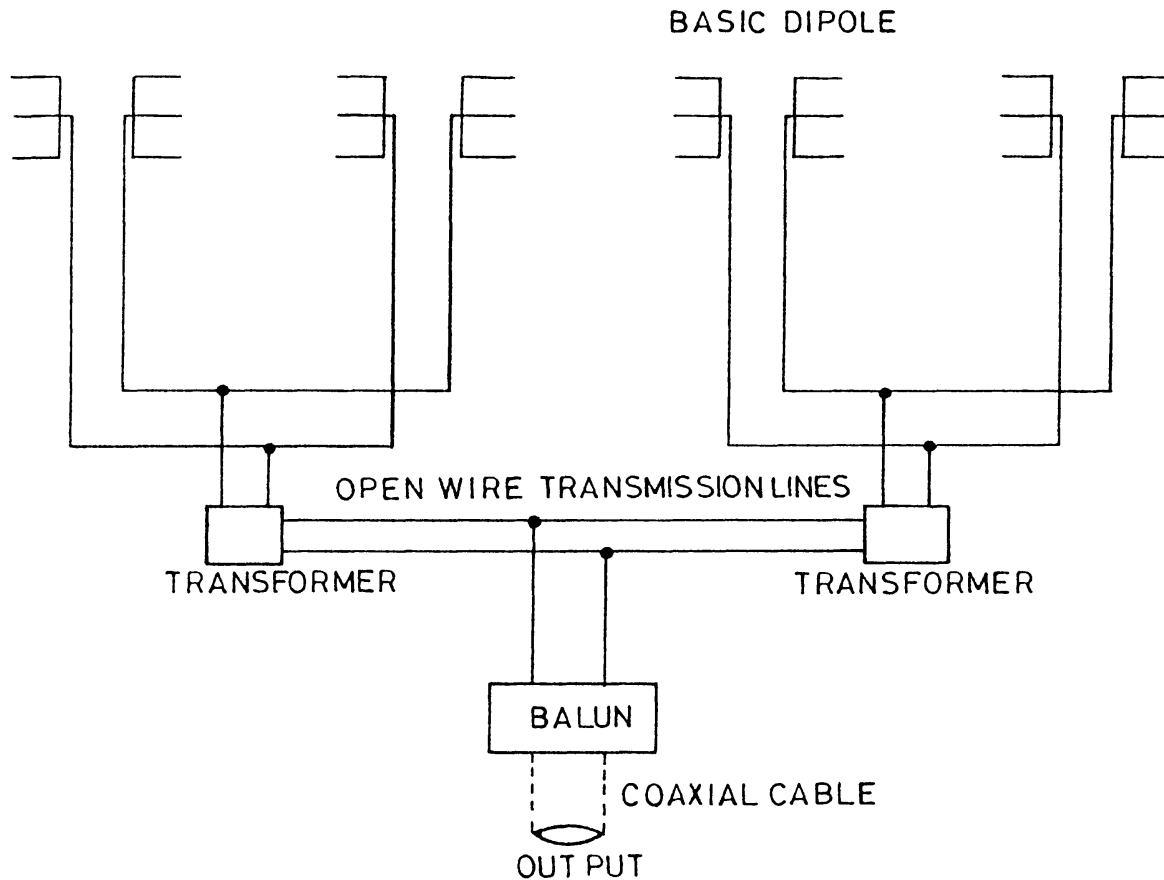


Fig. 2. A basic array element consisting of four dipoles connected in a branched feeder system.

The sum of the outputs of the north and south arrays can be multiplied with the E–W array to produce a beam of  $26' \times 20'$  (Sastry, 1989).

The E–W and the S antenna arrays were used for one-dimensional synthesis imaging of the accessible sky. For this purpose only one row of the E–W array is correlated with the outputs of each one of the 88 rows of the S array. The amplified outputs of the 88 rows of the S array are transmitted to the central observatory with 23 open wire transmission lines using time division multiplexing. The dipoles at the center of the E–W array are included in both E–W and S arrays in order to measure the zero spatial frequency component (Uday Shankar and Ravi Shankar, 1990).

The effective area of the telescope is approximately 20 000 square meters at 34.5 MHz. The mean sky brightness temperature at this frequency is about 10 000 K and so the minimum detectable flux density is of the order of 10 Janskys with an integration time of 10 s and a bandwidth of 200 kHz. The minimum detectable brightness temperature variations are about 1000 K. Aerial photographs of the E–W and S arrays are shown in Figure 7.

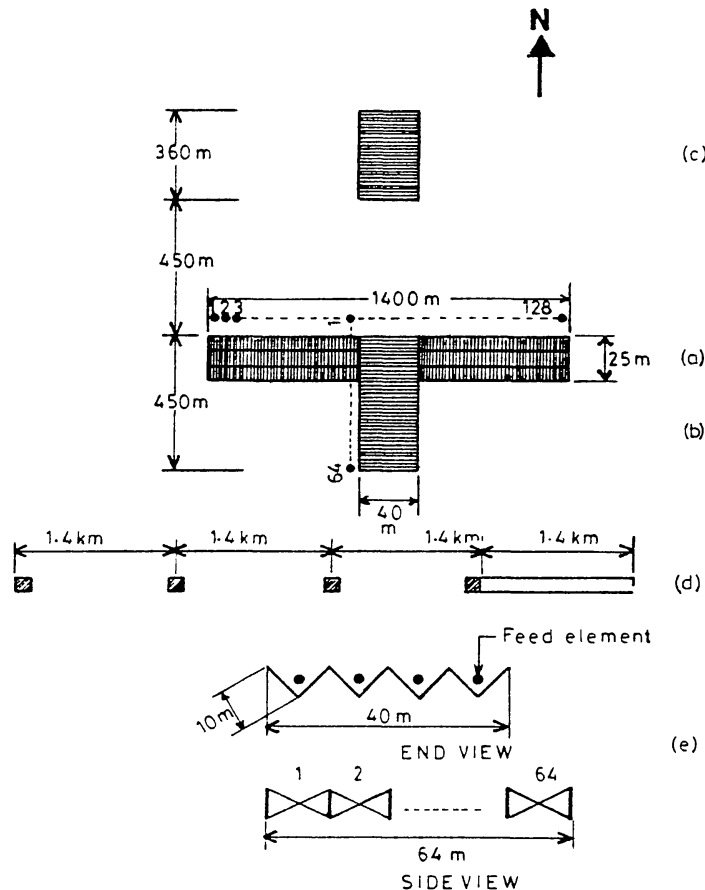


Fig. 3. Lay-out and dimensions of various antenna arrays at Gauribidanur (a) east-west array of GBDRT: 4 rows in N-S direction, 160 dipoles in each row; (b) south array of GBDRT; 90 rows in N-S direction, 4 dipoles in each row; (c) North array; 64 rows in N-S direction, 1 Yagi in each row; (d) compound grating interferometer: east-west array of GBDRT and 4 grating units. Each grating unit consists of 8 Yagis; (e) broadband array; 64 bi-conical dipoles arranged in a matrix of  $4 \times 16$  along E-W and N-S directions, respectively. The E-W and S arrays of the Radioheliograph are shown as filled circles in (a) and (b).

## 2.2. COMPOUND GRATING INTERFEROMETER

High-resolution one-dimensional observations are made with a compound grating interferometer with an E-W fan beam of 3 arc min at 34.5 MHz. It consists of four grating units placed at intervals of 1.4 km (length of the E-W array of the 'T') on a E-W base line starting from the western end of the E-W array as shown in Figure 3. Each grating unit consists of 8 Yagi antennas combined in a branched feeder system. The outputs of each one of the grating units is correlated with the E-W array output to synthesize the fan beam.

## 2.3. BROADBAND ARRAY

A broadband array usable in the frequency range 30 to 70 MHz, mainly for solar observations, is also available. The basic element of this array is a biconical dipole

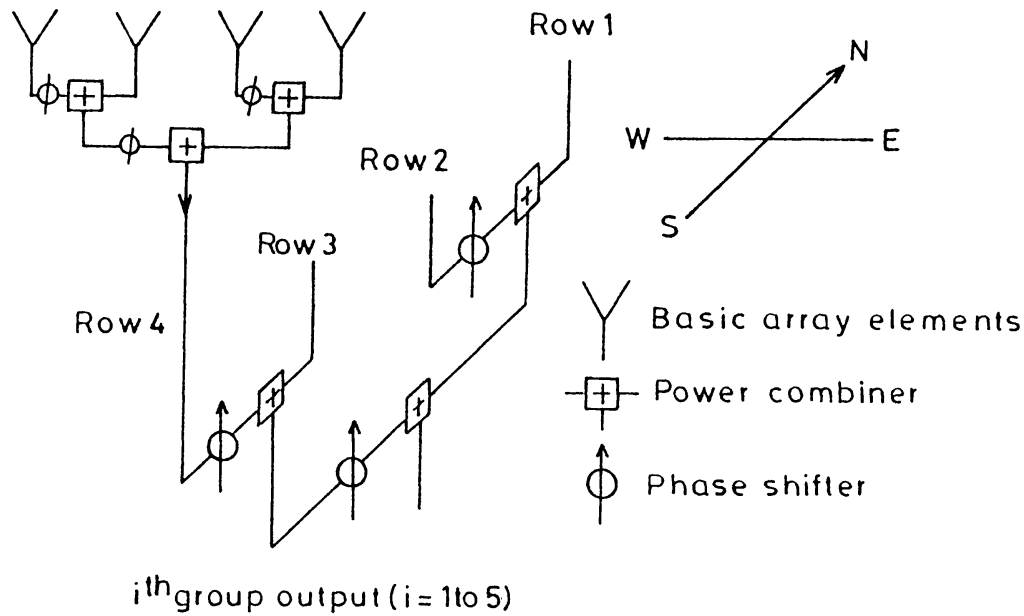


Fig. 4. Configuration within each east-west group.

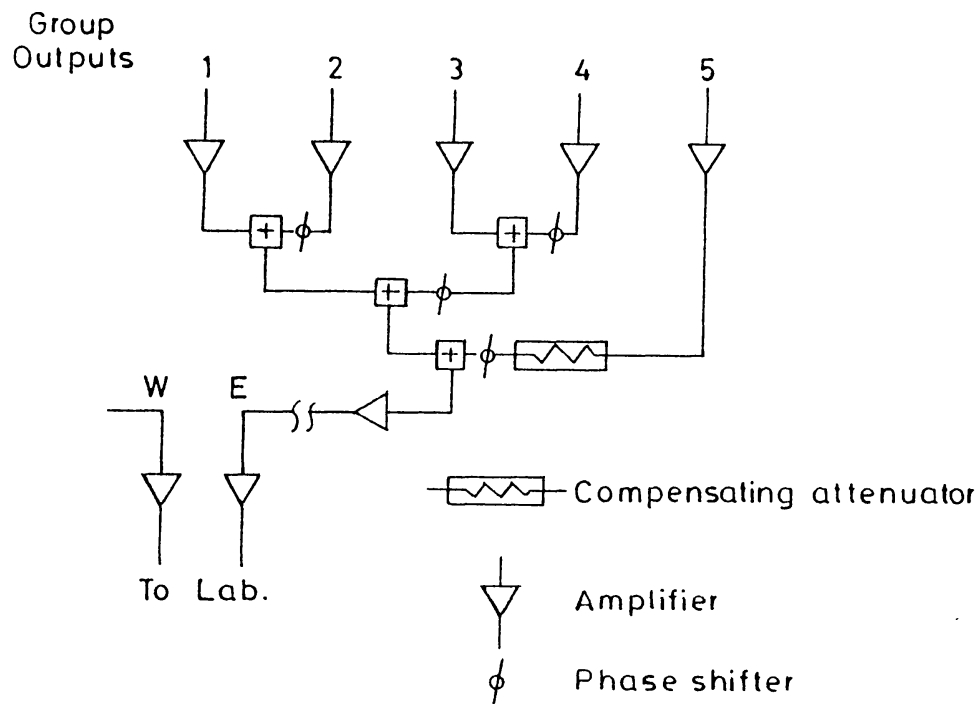
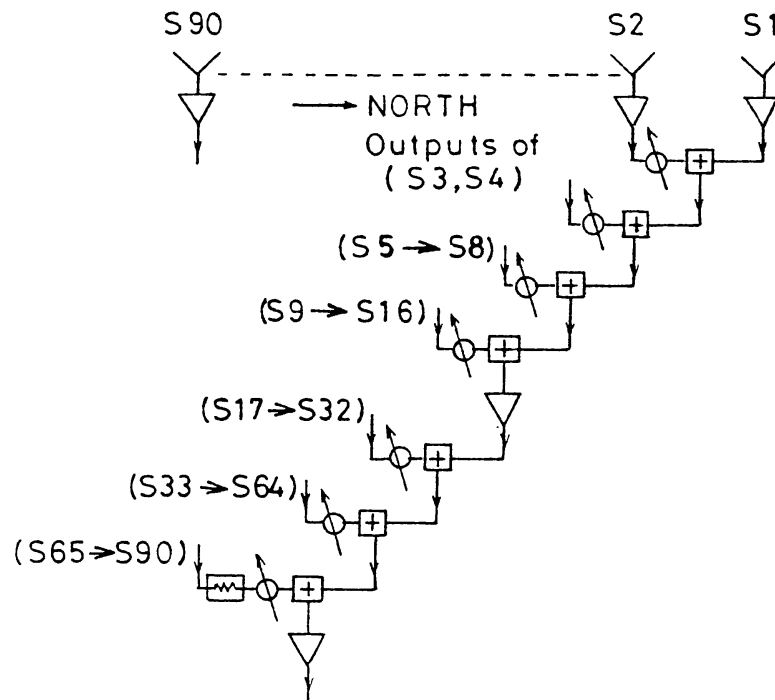


Fig. 5. Combination of groups in the east-west array.

with a VSWR  $\approx 2$  in the above frequency range. The array consists of 64 elements arranged in four groups of sixteen dipoles. Each group of sixteen dipoles is placed in a  $90^\circ$  corner reflector of size  $10 \times 64$  m as shown in Figure 3. The dipoles accept NS polarization and delay shifters are introduced at appropriate places to steer the beam in the NS direction within  $\pm 45^\circ$  of the zenith. The position of the beam



S Array output To Lab.

Fig. 6. Configuration of the south array.

formed is independent of frequency allowing simultaneous observation of a source over the full bandwidth of the system. This array is also used in the transit mode and the available observing times range from 26 minutes at 65 MHz to about an hour at 35 MHz. The effective area is 2000 square meters and the sensitivity obtainable is better than 100 Jy at 65 MHz for a bandwidth of 1 MHz and integration time of 1 s (Subramanian *et al.*, 1986).

#### 2.4. THE RADIOHELIOGRAPH

The Gauribidanur Radioheliograph will produce images of the solar corona at several frequencies in the range 40 to 150 MHz. The antenna system for the radioheliograph consists of two Log Periodic Dipole (LPD) arrays arranged in the form of the letter 'T' with the long arm, of length 1.2 km, along the E-W direction and the short arm, of length 0.45 km, along the south direction. The LPD is designed to operate in the frequency range 30 to 150 MHz with a VSWR < 2 and has a gain of 8 db. The beamwidth of the LPD is 60 in the E plane and 100 in the H plane. In the E-W arm 128 LPDs are arranged with an interelement spacing of 10 m. The E-W arm is divided into 32 groups of 4 elements each. The signal from each element is passed through a high pass filter with a cut off at 40 MHz and a broadband amplifier with a gain of 30 db and Noise Figure of 3 db. The outputs of the amplifiers are combined in a branched feeder system. In the south arm 64 elements are arranged with an interelement spacing of 7 m. The filtered and amplified outputs

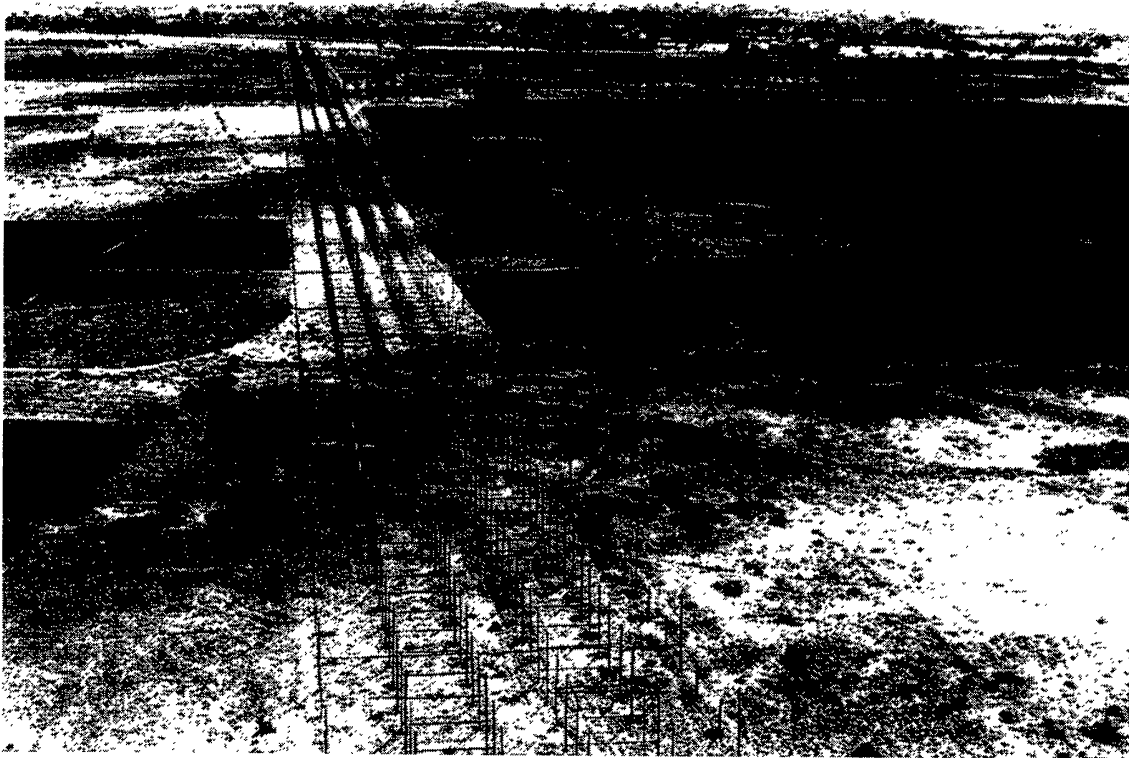


Fig. 7a.



Fig. 7b.

Fig. 7a-b. Aerial views of (a) east-west array, (b) south array of GBDRT.





Fig. 8a.



Fig. 8b.

Fig. 8a–b. Views of the (a) east–west array, (b) south array of the Radioheliograph at Gauribidanur.

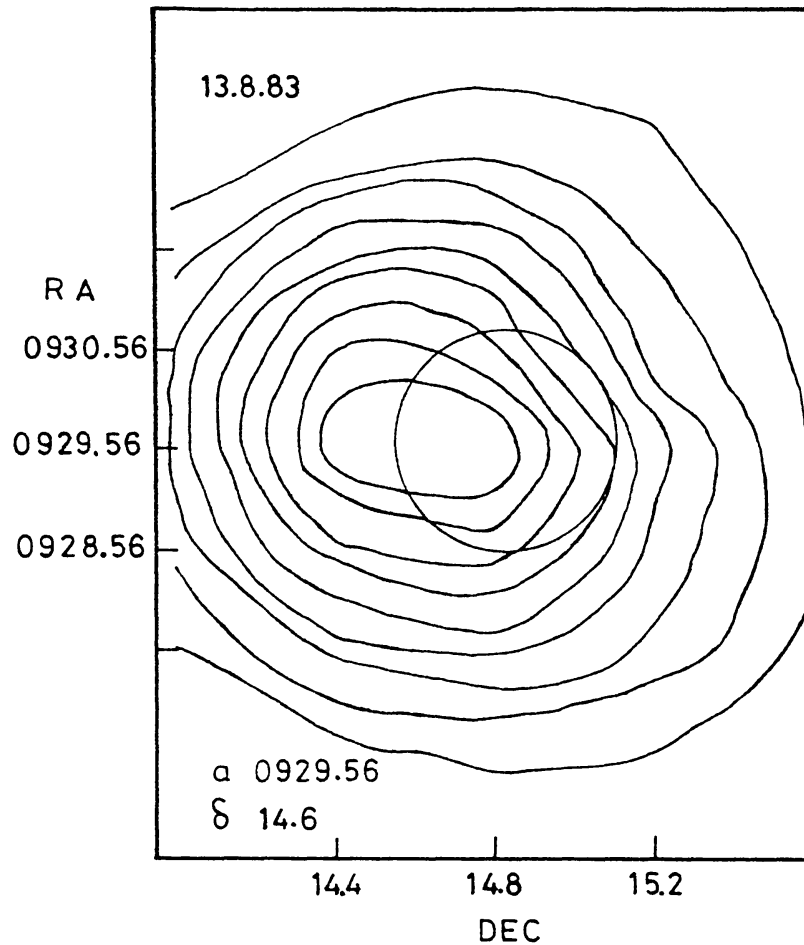


Fig. 9. A map of the quiet Sun made with the GBDRT at 34.5 MHz.

are combined using delay shifters, power combiners. Photographs of the completed E–W and S arms are shown in Figure 8 (Subramanian *et al.*, 1993).

## 2.5. RECEIVERS

The receiving systems available include several analog receivers and two digital correlators: one with 128 channels and the other with 64 channels. A 1024 channel digital correlation receiver will be available soon. The bandwidths and time constants of the analog receivers are selectable in the range 15 kHz to 1 MHz and 10 ms to 30 s, respectively. The 128 channel digital receiver is a double sideband system with one bit correlators. This receiver can also be configured as an auto-correlation spectrometer for spectral line and pulsar observations. The 64 channel digital correlator is meant for use with heliograph. An acousto-optic spectrometer (AOS) provides high temporal and frequency resolution for studies of the radio bursts from the Sun. The AOS has a bandwidth of 30 MHz with 1760 channels giving a frequency resolution of about 30 kHz. The spectrograph is interfaced via an A/D converter and a memory bank to VAX11/730 computer. All its 1760 chan-

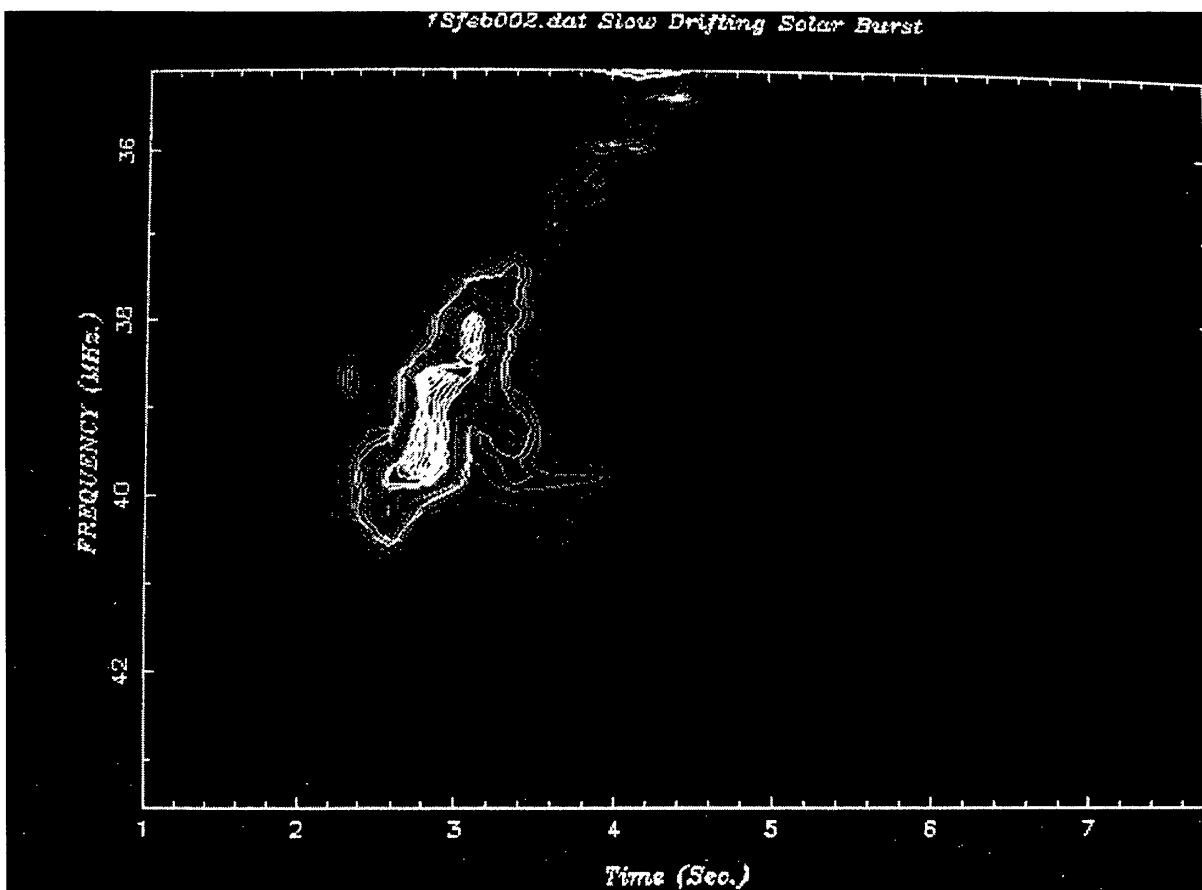


Fig. 10a.

Fig. 10a–b. Slow drift radio bursts recorded at Gauribidanur using the AOS and the broadband array. The burst shown at (a) started at 06:13:52 UT while that in (b) started 06:33:02 UT on February 13, 1990 during solar storm period. The drift rates of the bursts are  $2.40 \text{ MHz s}^{-1}$  and  $1.12 \text{ MHz s}^{-1}$ , respectively. The intensity levels show progressively increasing radio flux from the outer contour to the inner.

nels are scanned every 250 ms and the data are recorded either on the user disk of the computer or magnetic tape units.

### 3. Observations and Results

The telescopes are being used for observations of the Sun, galactic sources, background survey and extragalactic sources.

#### 3.1. SUN

The decameter wave radio telescope was used to produce maps of the continuum emission from the undisturbed Sun and active regions. These are the first maps of this kind made anywhere in the world. These observations were used to show that

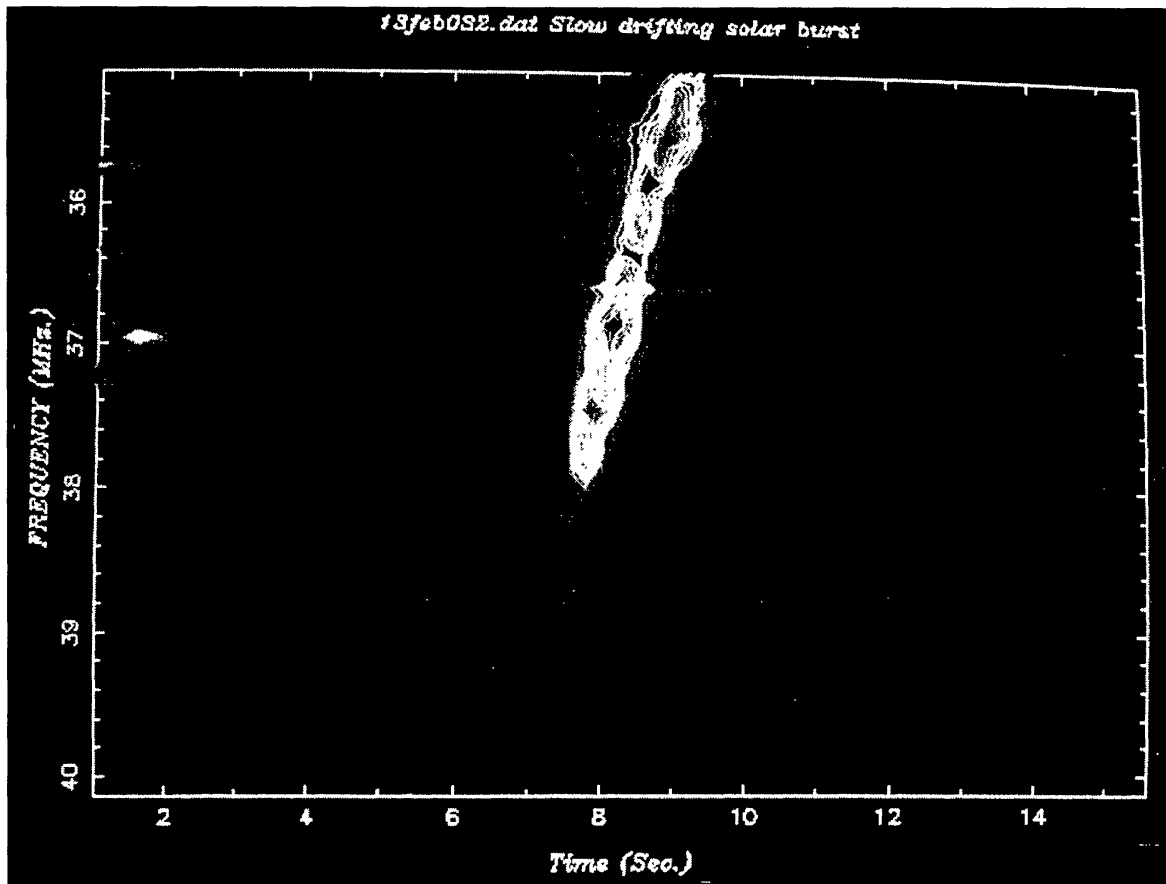


Fig. 10b.

the peak brightness temperature of the undisturbed Sun could be  $\leq 0.2 \times 10^6 \text{K}$  and also can vary by a factor of two to three on consecutive days. It was also found that the variations in brightness temperature can be very large ( $>$  factor of six) in a period of two to three weeks although there is no apparent contribution from active regions. The variations of the brightness temperature and half power widths of the radio Sun are not correlated. It is therefore suggested that the temperature variations are not caused by either uniform density variations or due to scattering by an irregular corona (Sastry *et al.*, 1981a, 1983; Sastry, 1994). A typical map of the Sun obtained during the Sunspot minimum period 1983 are shown in Figure 9. The compound grating interferometer was used to make one dimensional scans of the Sun at 34.5 MHz with a resolution of 3 arc min. This is the highest resolution ever used to make scans of the Sun at such a low frequency. These scans are used to measure the variations in the E-W diameter of the undisturbed Sun, active regions and coronal holes (Sastry, 1994). The acousto-optic spectrometer along with the broadband array is being used to study solar and Jupiter radio bursts with high temporal and frequency resolution. Several interesting structures in solar radio bursts are detected. Bursts with short duration and occurring only in a small

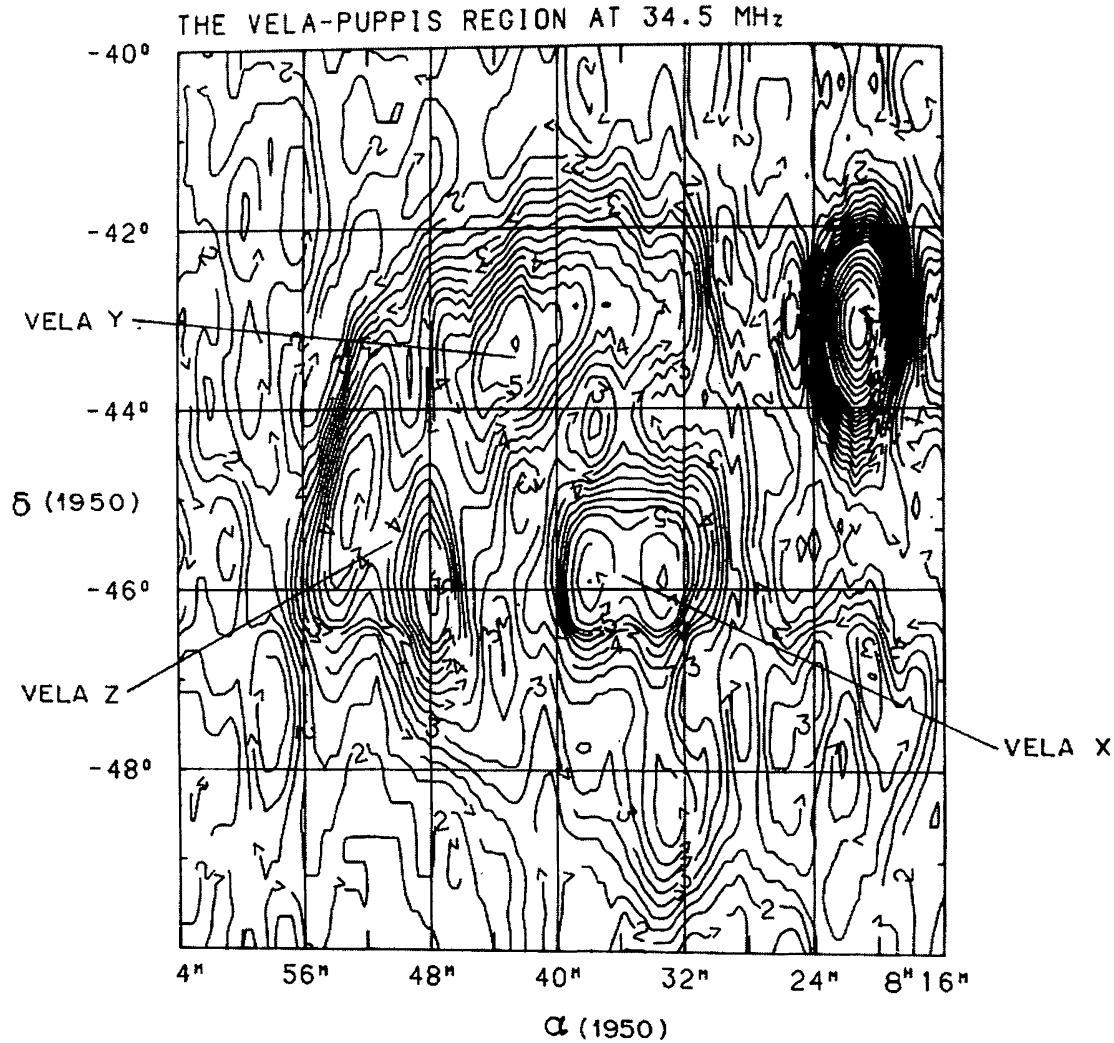


Fig. 11. A 34.5 MHz map of the Vela-Puppis region. the resolution is  $26' \times 84'$  along R.A. and Dec, respectively. The contours are labelled in  $10^4$  K.

frequency range but similar to the well known Type II bursts in drift rates and other characteristics are shown in Figure 10 .

### 3.2. GALACTIC SOURCES

#### 3.2.1. *Supernova Remnants*

The telescope has been used to study the structure of extended supernova remnants at decameter wavelengths like Cygnus Loop, IC443, HB9, Vela XYZ, etc. (Sastry *et al.*, 1981b; Dwarakanath *et al.*, 1982; Dwarakanath, 1991). The integrated low-frequency flux densities are measured and the variations in spectral indices across some of these remnants are determined. The reduction in flux density in some cases is shown to be due to absorption in the interstellar medium. In the case of Vela XYZ the spectral index estimates along with other known characteristics strengthen the earlier hypothesis that Vela X is plerion while Vela YZ is a shell-type supernova remnant. A 34.5 MHz map of Vela-Puppis region is shown in Figure 11.

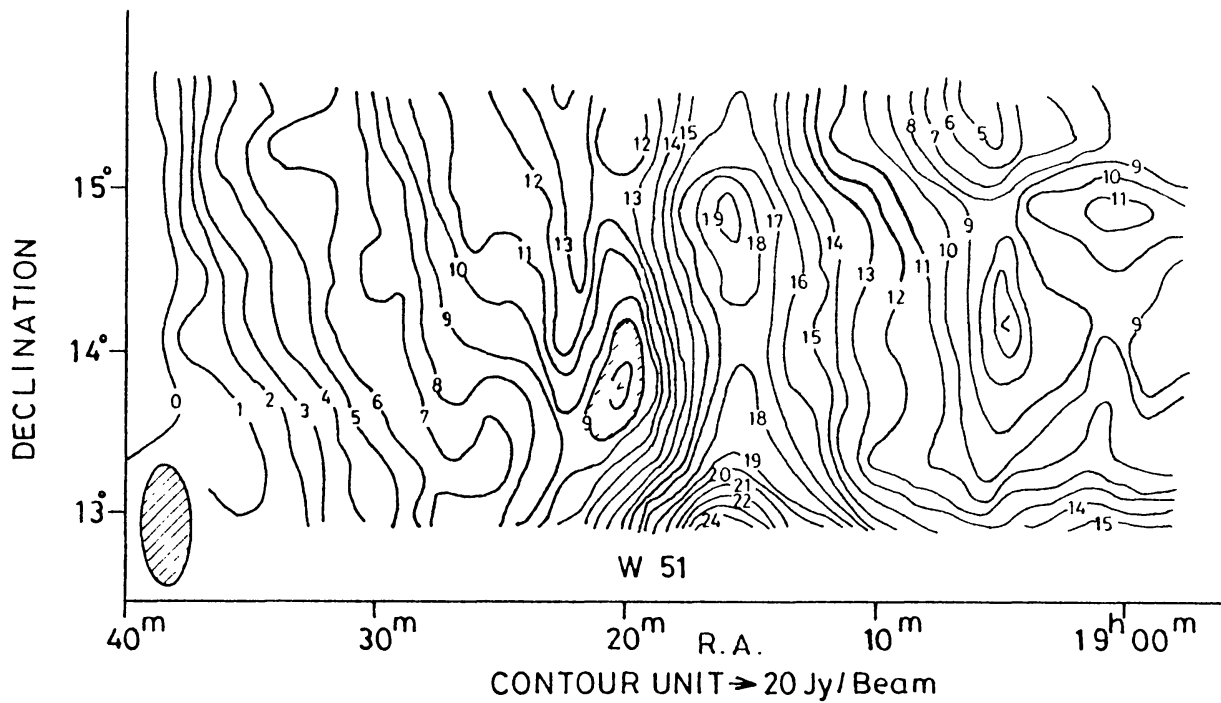


Fig. 12. A 34.5 MHz map of the galactic plane around the HII region complex W51 made with GBDRT.

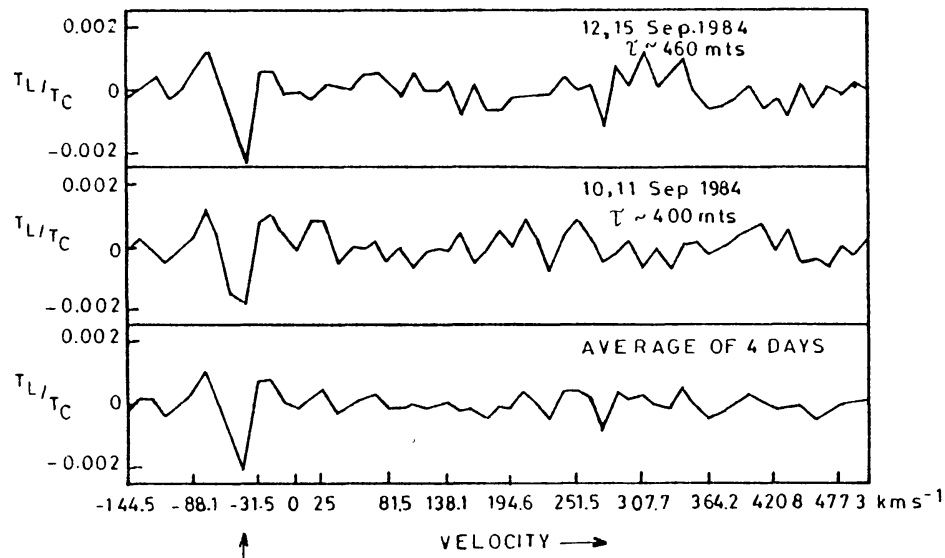


Fig. 13. The summed profile of the carbon recombination lines  $C574\alpha$  and  $575\alpha$  detected in the direction of Cas A at  $44 \text{ km s}^{-1}$ . Since the emission of Cas A dominates the system temperature, the optical depth ( $\tau$ ) is very close to the measured ratio of line to continuum temperature ( $T_l / T_c$ ).

### 3.2.2. Ionized Hydrogen Regions

The decameter wave radiotelescope is the most sensitive detector of ionized hydrogen regions (H II) in the galaxy. The electron temperature of these regions is usually  $<10\,000 \text{ K}$  and so they appear as continuum absorption features against the very

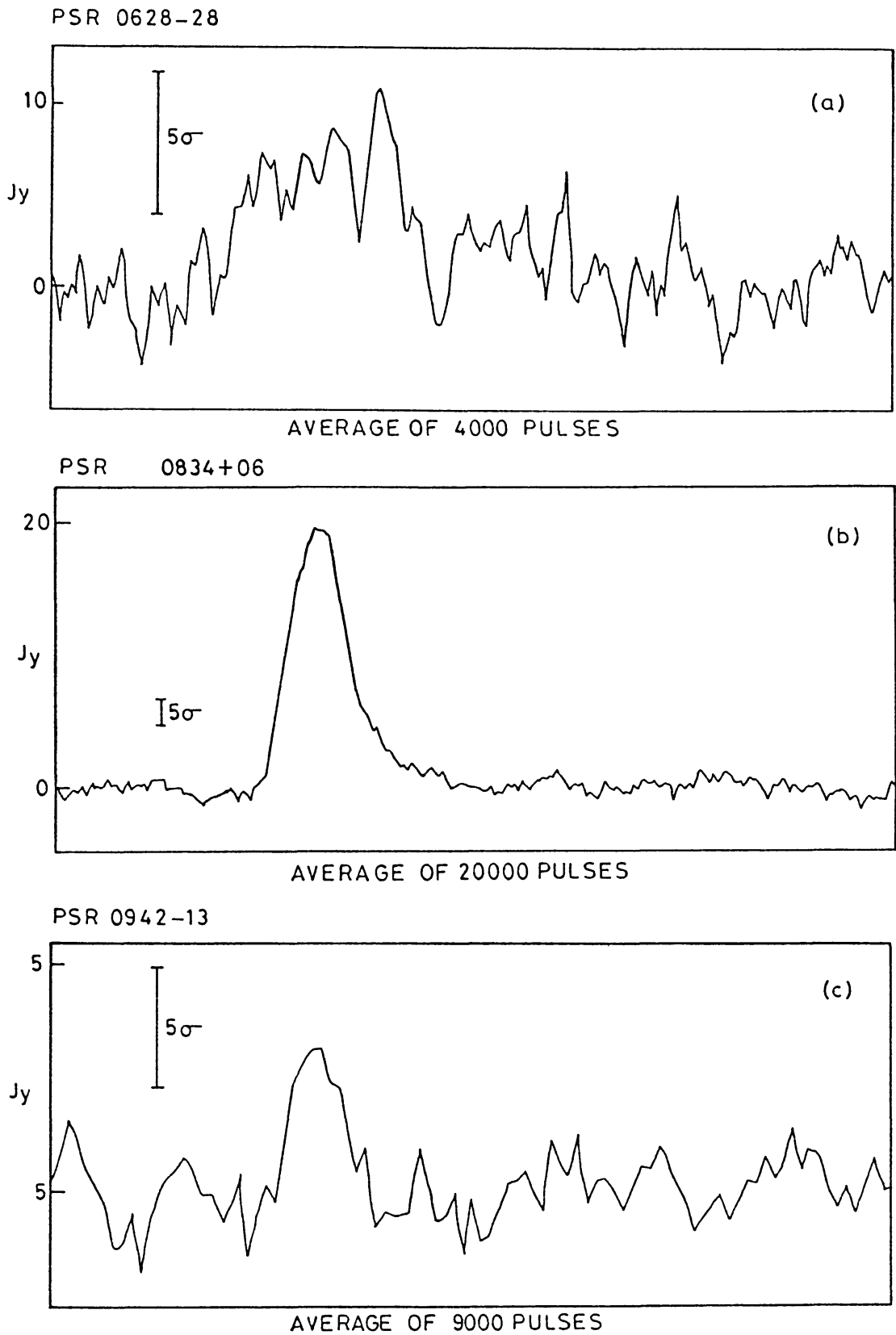


Fig. 14a-c.

Fig. 14a-g. The average time profiles of seven pulsars at 34.5 MHz obtained with the GBDRT using the single channel scheme. The error bars correspond to five times the r.m.s noise deviation.

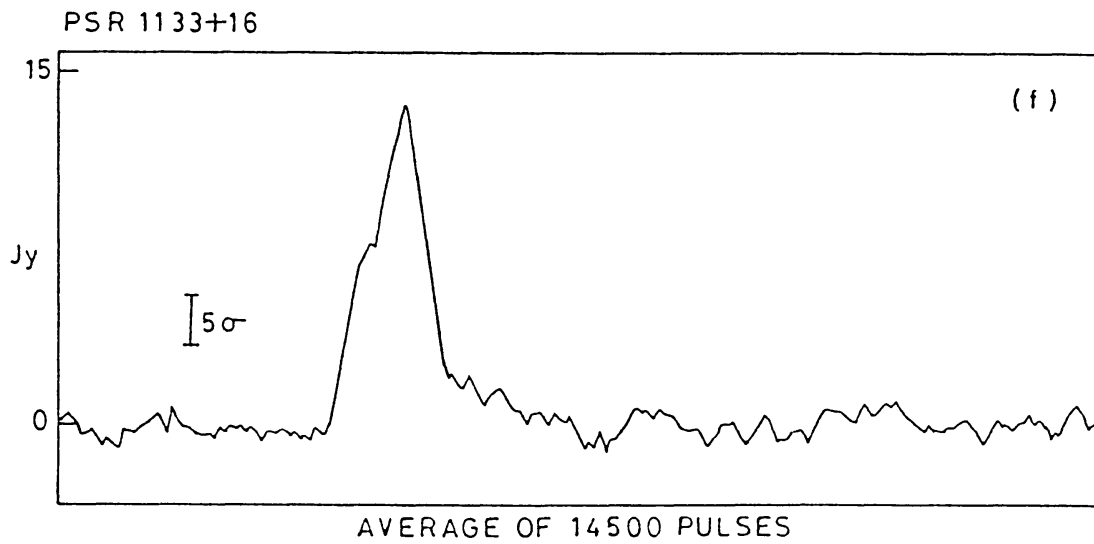
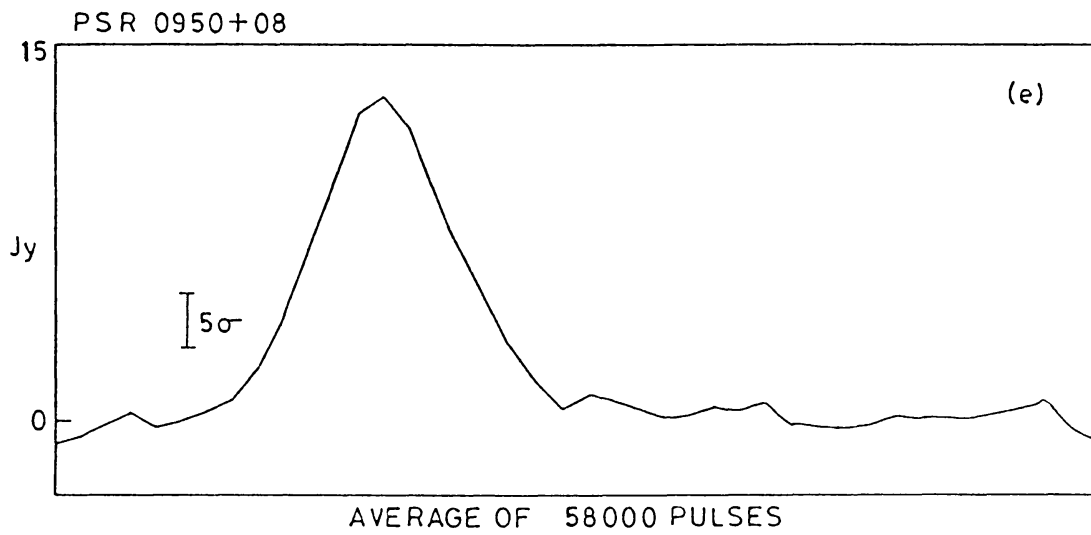
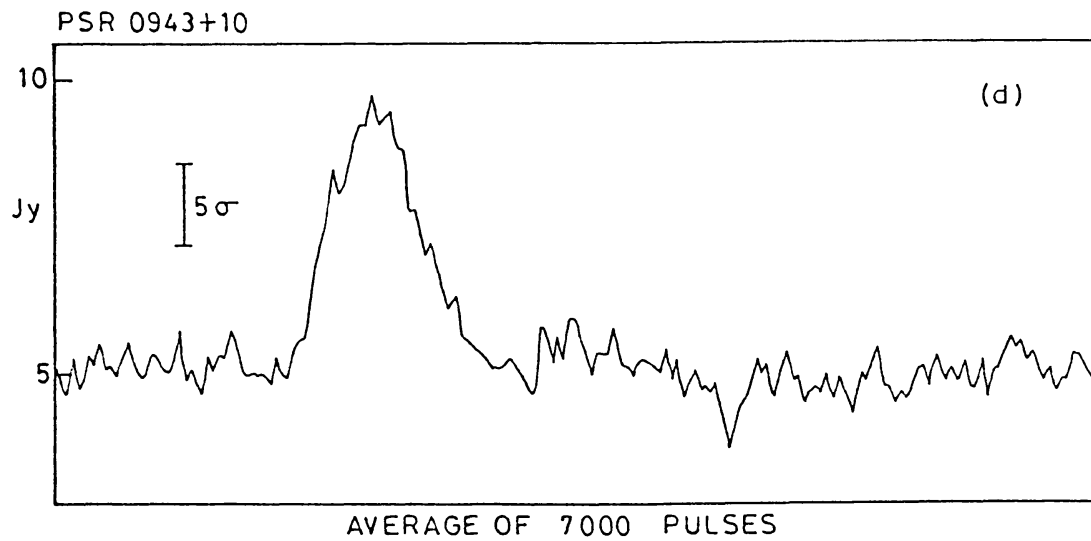


Fig. 14d-f.



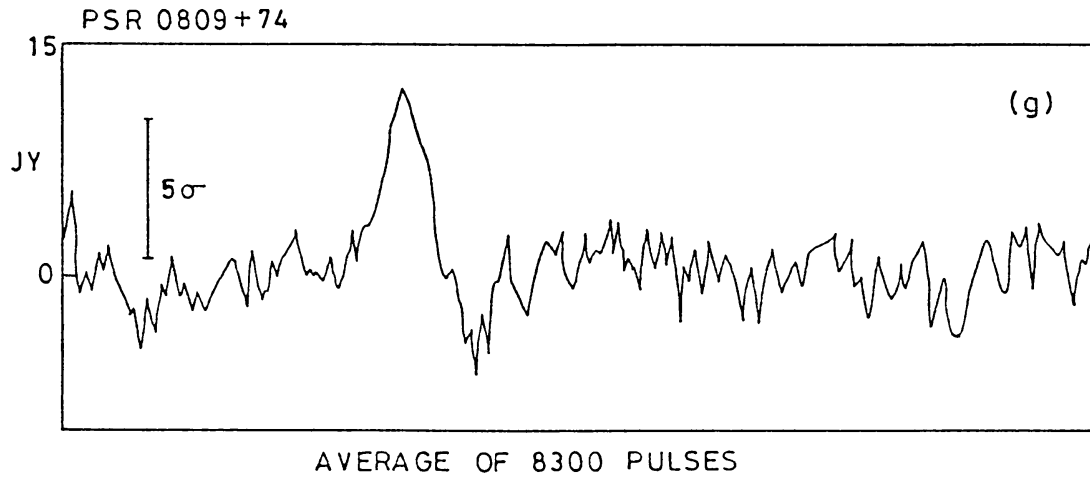


Fig. 14g.

bright non-thermal background radio emission from the galaxy. It is possible to measure the electron temperature of the H II regions directly unlike high frequency measurements where one has to assume LTE conditions in the nebula to derive the temperatures. Nearly 30 discrete absorbing regions are detected, the prominent among them being Rosette Nebula and W 51 complex. It is shown that the absorptions must be due to nearby ( $<3$  kpc), extended (20 to 100 pc) and low density ( $10 \text{ cm}^{-3}$ ) H II regions. In the case of Rosette Nebula the possibility of the existence of a temperature gradient across the nebula is pointed out. It is also shown that the complex W51 is surrounded by a non-thermal ring which is probably a supernova remnant (Deshpande *et al.*, 1984b; Deshpande and Sastry, 1986). A 34.5 MHz map of the galactic plane around W51 complex is shown in Figure 12.

### 3.2.3. Recombination Lines

The 128 channel digital correlator is used in the autocorrelation spectrometer mode along with the south array to search for recombination lines in absorption in the direction of strong radio sources. The  $C574\alpha$ , and  $C575\alpha$  lines detected in the direction of Cas A are shown in Figure 13 (Uday Shankar and Ravi Shankar, 1990). At present the autocorrelation spectrometer is being modified to observe simultaneously eight adjacent spectral lines around 34.5 MHz.

### 3.2.4. Pulsars

The behavior of pulsars at low radio frequencies ( $<50$  MHz) is not well understood due to very limited observational data on pulsars at these frequencies. The decameter wave radiotelescope is used to detect pulsars with high sensitivity and time resolution at a frequency of 34.5 MHz (Deshpande *et al.*, 1984b). These observations are initially made with a single frequency analog correlation receiver using the tracking facility. The data processing consists of folding over a two period stretch and testing for significant detection of two similar pulses separated by one

PSR 0628-28

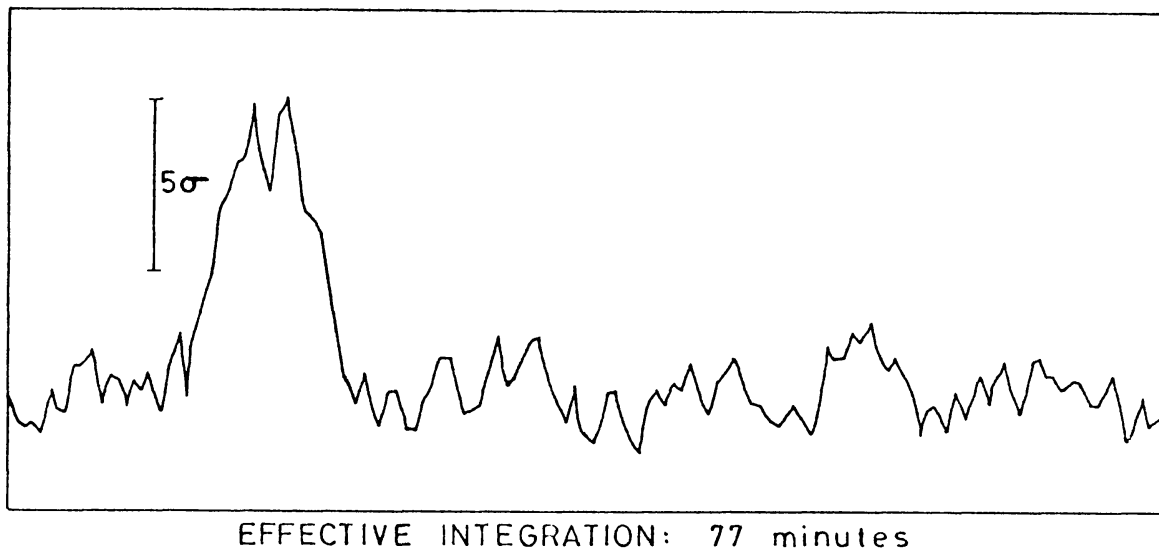


Fig. 15a.

PSR 1919+21

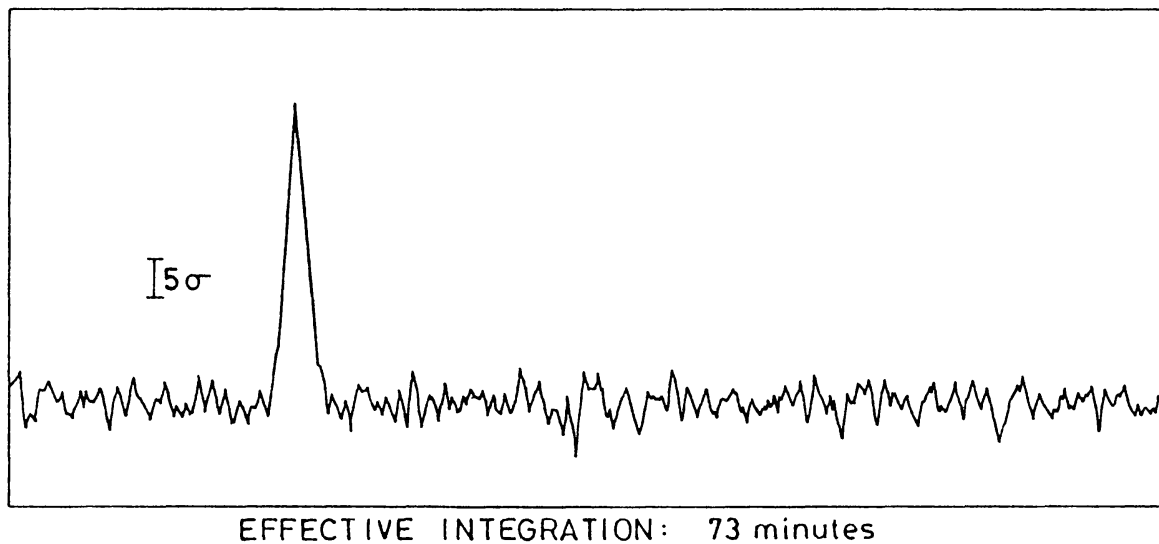


Fig. 15b.

Fig. 15a-b. The average time profiles of two pulsars obtained with swept frequency dedispersion scheme.

period. To improve the S/N ratio data from different days were averaged. Subsequently a digital correlation receiver and a swept frequency local oscillator system were employed. The local oscillator was swept over the bandwidth of the receiver at a rate given by the dispersion measure of a given pulsar and the autocorrelation function(ACF) was measured. The power spectrum is obtained from the ACF and

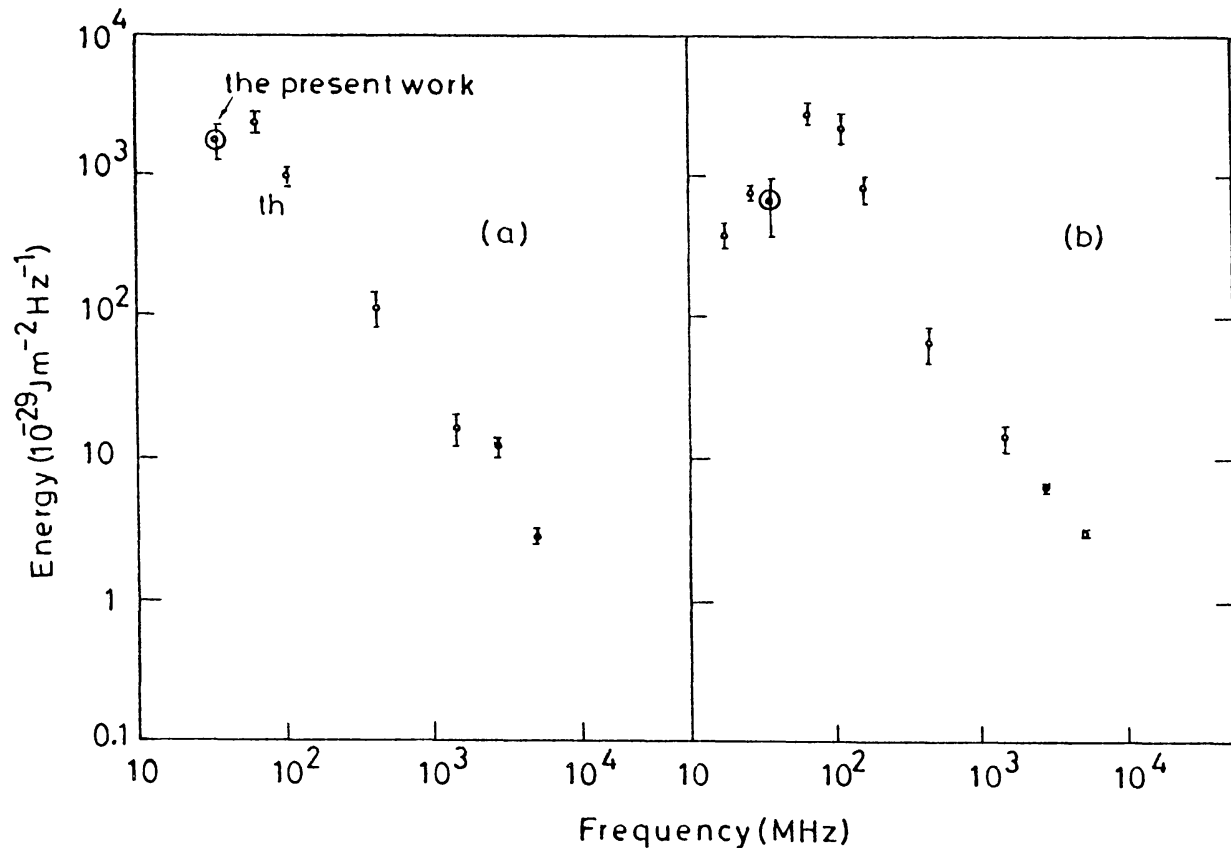


Fig. 16a-b.

Fig. 16a-g. The average pulse energy spectra of six pulsars over the radio frequency range. The points indicated by an extra circle correspond to the present measurements.

then an appropriate dispersion law is used to convert the spectral pattern into a time domain pattern. Observations are made on 20 known pulsars and 8 are detected. The average profiles obtained for seven of these pulsars, using the single channel scheme, are shown in Figure 14. These profiles are affected mainly by dispersion smearing over the 30 kHz bandwidth used and so some structure is lost. The average profiles obtained by the swept frequency dedispersion scheme for the two pulsars PSR 0628-28 and PSR 1919+21 are shown in Figure 15. Three pulsars, namely PSR 0628-28, PSR 0942-13 and PSR 0943+10 have been detected for the first time at a decametric wavelength. The average energy spectra for six of the detected pulsars is shown in Figure 16. Out of the three new detections at 34.5 MHz only in one case (PSR 0943+10) does the spectrum not appear to have a turnover down to 34.5 MHz. Such a spectrum would be of great interest if this trend continues to even lower frequencies. No significant interpulse emission beyond the main pulse window is detected for any of these pulsars. It is also shown that it is feasible to study the fluctuation spectra and slow variability at low frequencies (Deshpande and Radhakrishnan, 1992; Deshpande, 1992).

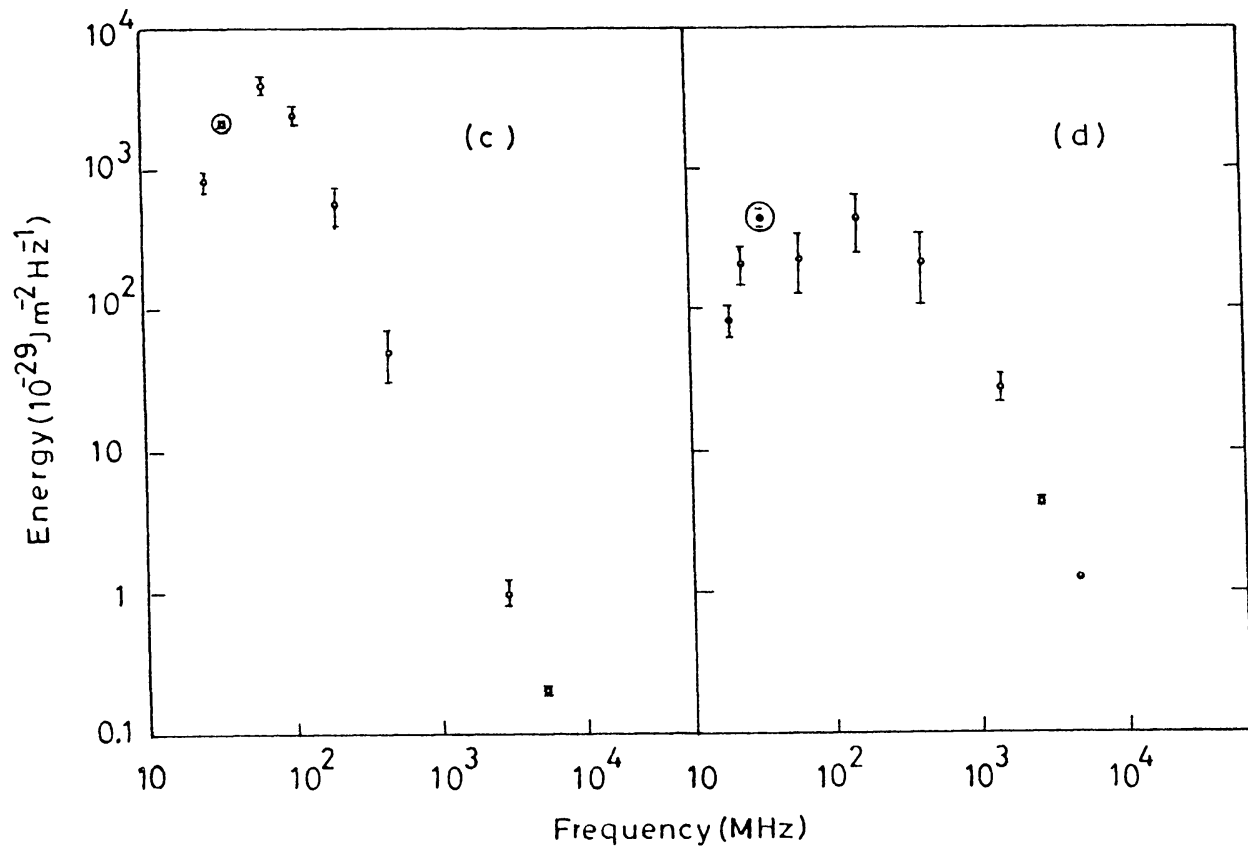


Fig. 16c-d.

### 3.2.5. A Synthesis Map of the Sky

The decameter wave radio telescope is used to make a synthesis map of the entire observable sky from Gauribidanur. For this purpose the telescope is used in the transit mode and a one dimensional synthesis is performed in the north-south direction. The survey covers the declination range  $-50^\circ$  to  $+70^\circ$  and the complete 24 hours in right ascension. The synthesized beam has a resolution of  $26' \times 42'$  ( $\delta = 14.1^\circ$ ). The sensitivity of the survey is  $5 \text{ jy beam}^{-1}$  ( $1\sigma$ ). Special care has been taken to ensure that the antenna responds to all angular structures and the surveys suitable for studies of both point sources and extended objects. A map of the region around galactic center is shown in Figure 17 (Dwarakanath and Uday Shankar, 1990).

### 3.2.6. Extragalactic Sources

One of the most interesting observations made with the decameter radio telescope in the study of extragalactic sources is the mapping of the diffuse radio emission from the halo of the Coma cluster of galaxies for the first time at a low frequency (34.5 MHz) with reasonable resolution (Sastry and Shevgaonkar, 1983). The observation of intergalactic matter is of great importance in astrophysics since it provides the gravitational forces necessary to bind together clusters of galaxies

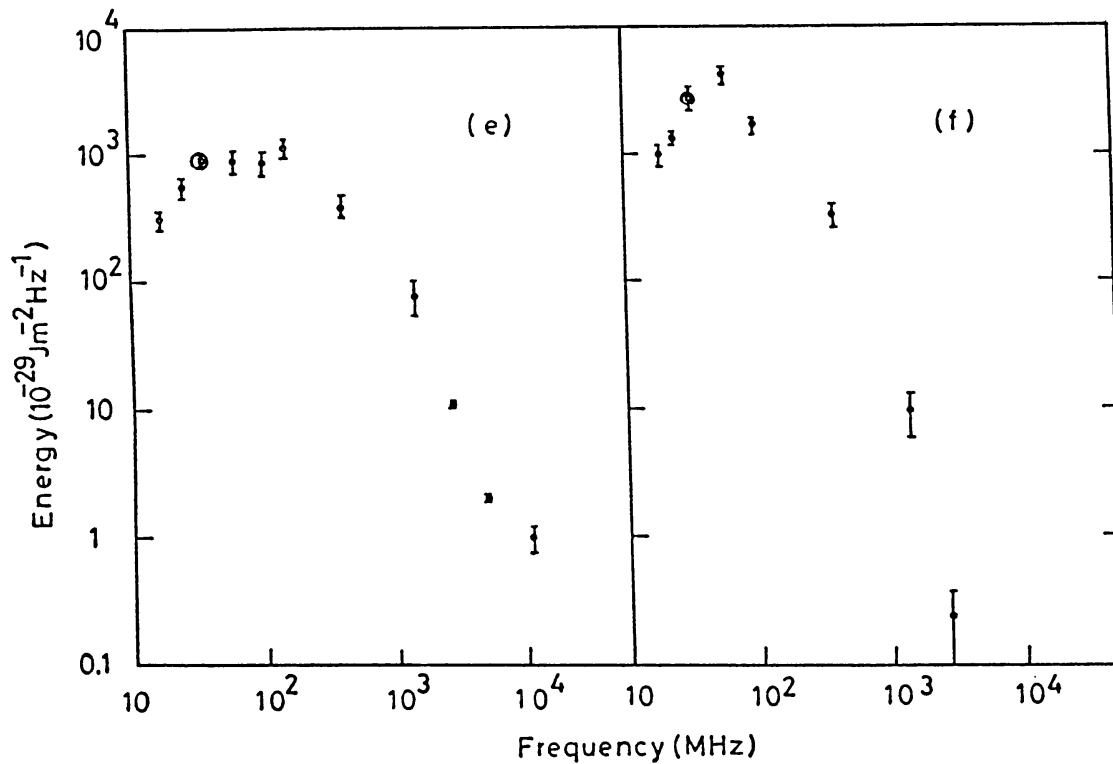


Fig. 16f-g.

and indeed the entire universe. The observed luminosity of the diffuse source is  $10^{41} \text{ ergs}^{-1}$ . The magnetic field in the intergalactic of the Coma cluster can be estimated by the minimum energy condition in which the magnetic energy density is equal to the particle energy density and is approximately equal to 2 microgauss. This indicates that relativistic electrons must have been ejected from the radio galaxies in the cluster at a mean rate of  $10^{51} \text{ erg yr}^{-1}$  for the 3.5 billion years. A map of the region around Coma cluster is shown in Figure 18.

#### 4. India-Mauritius Radiotelescope

The Raman Research Institute, University of Mauritius and the Indian Institute of Astrophysics in a joint collaboration program built a large meter wave synthesis radiotelescope on the island of Mauritius. This telescope is located at Bras d'eau in the north-east of Mauritius.

The radiotelescope is of the aperture synthesis type and is operated at a frequency of 150 MHz ( $\lambda = 2 \text{ m}$ ). This frequency is low enough to reveal absorption effects due to H II regions and at the same time reasonably high resolution can be obtained with moderate structures. The radiotelescope consists of a fixed east-west array of length 2 km and 16 movable arrays on a railway track of length of about 1 km in

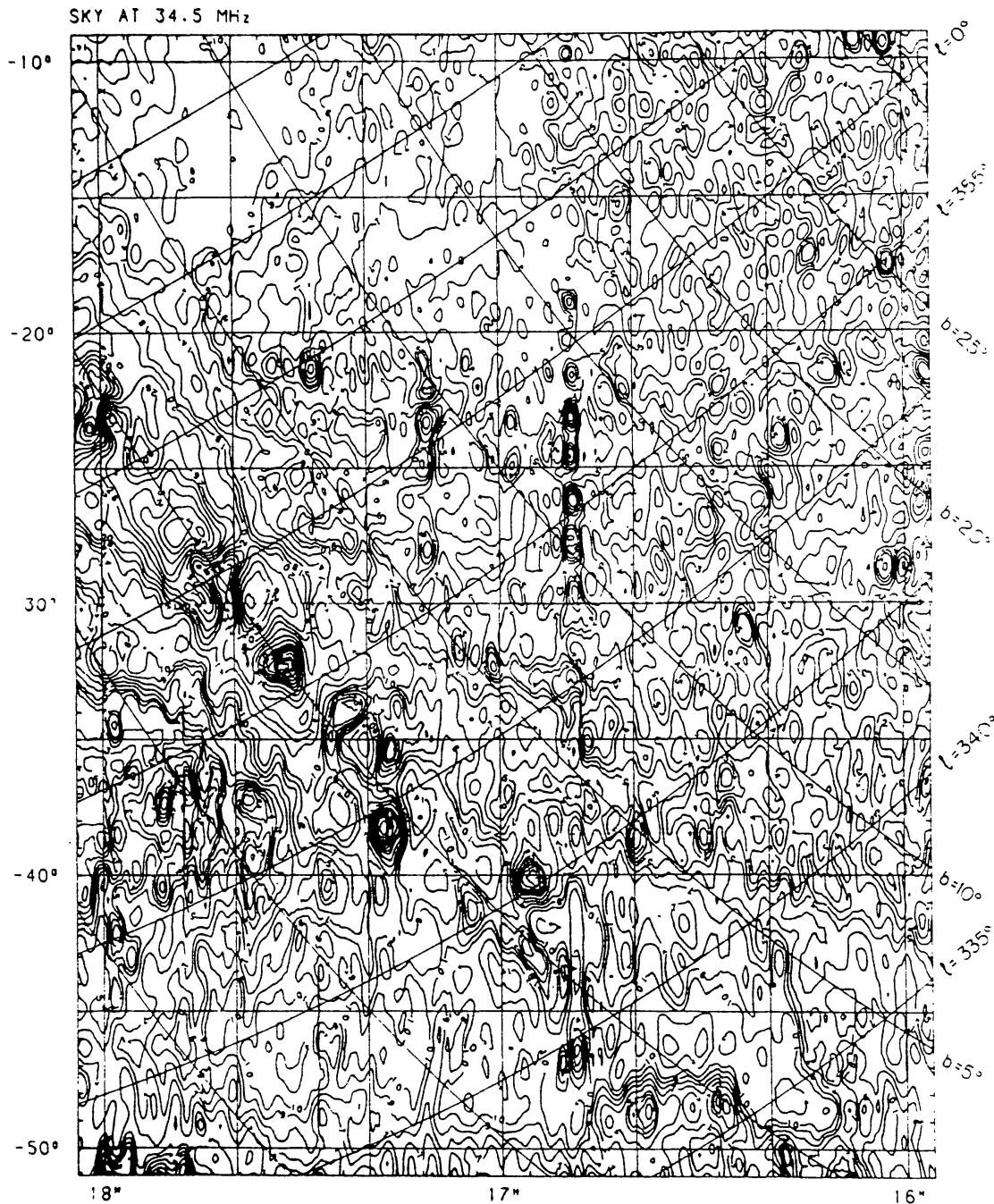


Fig. 17. A radio map of the galaxy within the range  $-10^\circ$  to  $-50^\circ$  Dec and 16:00 hr to 18:00 hr R.A. at 34, 5 MHz made with the GBDRT. The numbers on the contours are in units of 5722 K (full beam brightness temperature). Arrows on the contours which point clockwise enclose minima while those that point anti-clockwise enclose maxima. The synthesized beam has a resolution of  $26' \times 42' s$  ( $\delta - 14.1^\circ$ ).

a southerly direction from the center of the E-W array . The outputs of the E-W and each one of the movable arrays is correlated to synthesize a beam of about  $3'$  at 150 MHz.

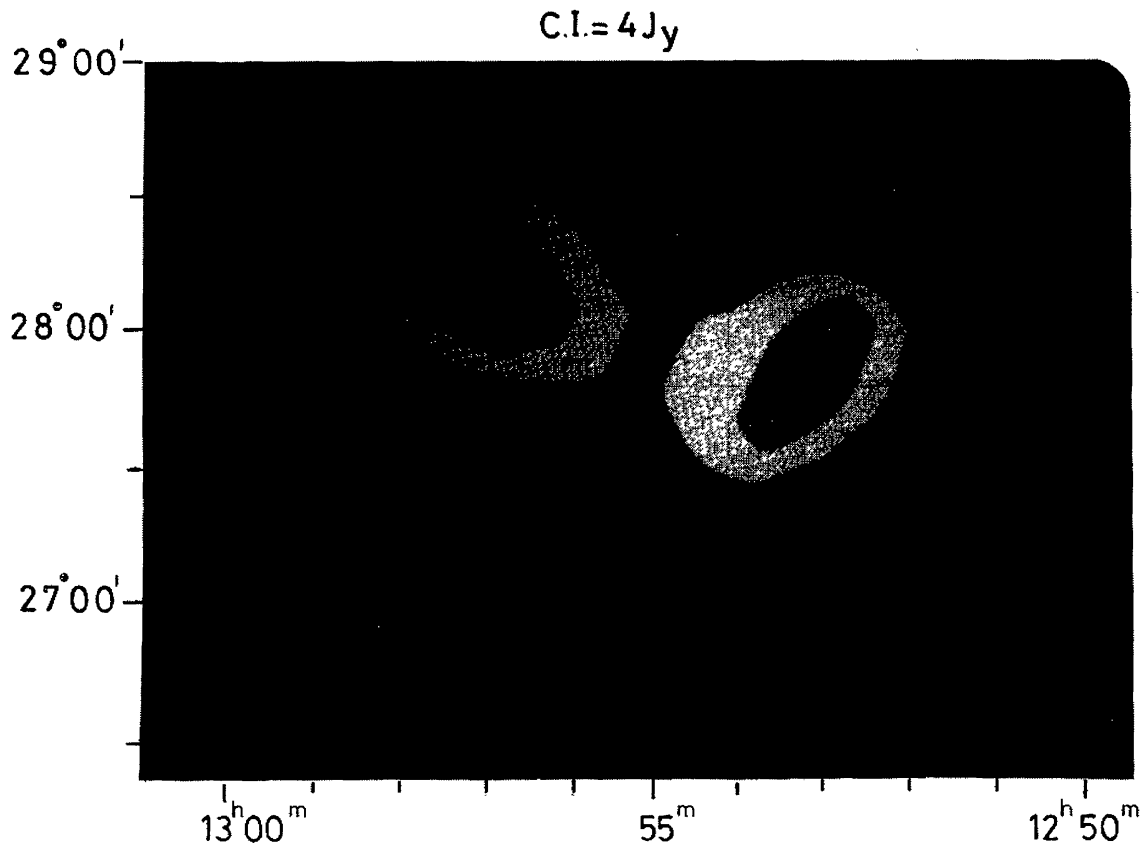


Fig. 18. A map of the region around Coma cluster of galaxies at 34.5 MHz made with the GBDRT. The position of the radio galaxy Coma A is shown by a cross.

The basic element of the array is a three turn helix of diameter 0.75 m and spacing between turns of 0.54 m. The design is suitable for the frequency range 100 to 200 MHz, although the dimensions are optimized at 150 MHz. The collecting area of the helix is  $\approx \lambda^2$  and the half-power beam width is  $\approx 55^\circ$ .

The E–W array consists of 32 groups of antennas and in each group there are 32 helixes. These are placed over a stainless steel reflector mesh of grid size  $2'' \times 2''$ . The helixes in each group are connected in a branched feeder system with low noise amplifiers at appropriate places to overcome losses and preserve signal to noise ratio. The combined output of the 32 helixes in each group is further amplified, down converted to 30 MHz (IF) and transmitted to the central observatory building through a 1 km length coaxial cable. Thus, there are 32 IF signals available at the central observatory from the E–W array. Due to the topography of the site the 32 E–W groups are not at the same height.

The south array consists of 16 mobile groups moving on a railway track of length 1 km. The railway track is laid in a southerly direction from the center of the E–W array. Each mobile group consists of four helixes on a movable platform and connected in a branched feeder system. These can be moved on the railway track to any position within 1 km of the center of the E–W array. The signals from the

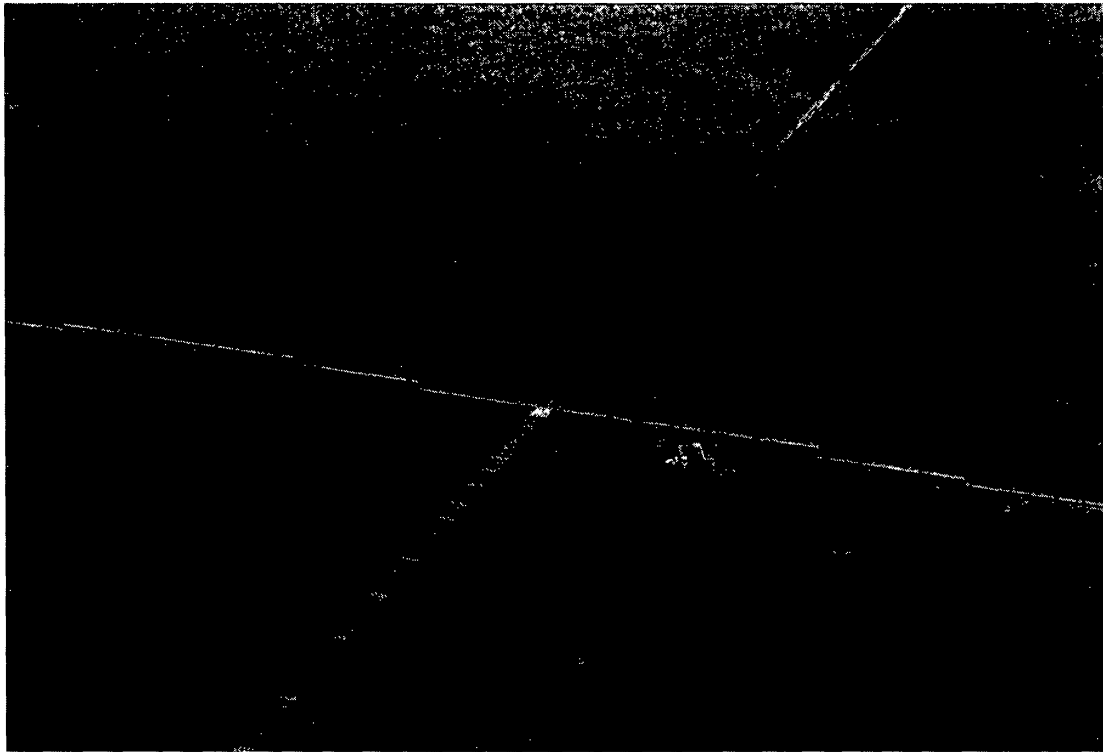


Fig. 19a.

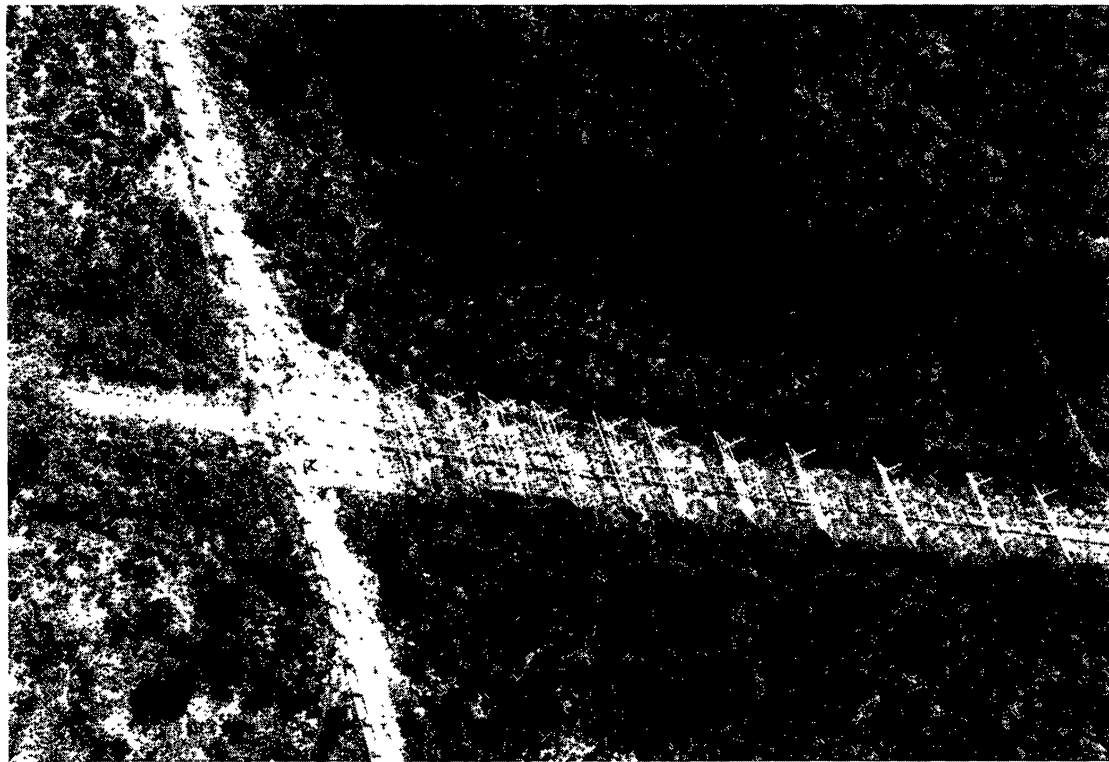


Fig. 19b.

Fig. 19a–b. Aerial view of the E–W and S arrays of the India–Mauritius Radiotelescope.



mobile arrays are amplified in the field in low noise amplifiers and down converted to 30 MHz (IF) and sent to the central observatory via 1 km length coaxial cables. Thus there are 16 IF signals available at the central observatory from the south array.

A 1024 channel digital correlator receiver originally built at the Clark Lake Radio Observatory of the University of Maryland, U.S.A. is given to this project by Prof. W. C. Erickson. This receiver uses the custom built integrated correlation chips VLA 1 and 2 developed for the National Radio Astronomy Observatory's Very Large Array also in U.S.A. The whole system is modified to suit the present purpose. The system permits simultaneous measurement of the complex visibility functions on 512 base lines. After Fourier transformation these visibilities yield a  $32 \times 32$  element picture of the area of the sky under observation with a resolution of about 3 arc min. Aerial views of the E–W and South arrays of the India–Mauritius Radiotelescope are shown in Figure 19.

This telescope was inaugurated by the Hon'ble Prime Minister of Mauritius on November 4, 1992. Observations of the region around galactic center are being made and the results will be published separately.

### Acknowledgements

I would like to thank Late Prof. M. K. Vainu Bappu for his encouragement and kind support without which the low frequency radio astronomy project at Gauribidanur, India would not have existed. I would also like to thank Prof. V. Radhakrishnan for his advice, interest and support without which the project would not have progressed. The India–Mauritius Radio Telescope owes its existence to the kind support of Prof. V. Radhakrishnan. Messrs M. Modgekar, A. T. H. Hameed, G. N. Rajasekhara, Nanje Gowda, and H. Aswathappa have helped in the construction and maintenance of the radiotelescopes and also in the collection of the data.

The work reviewed here is done primarily by my colleagues, R. K. Shevgaonkar, A. A. Deshpande, K. S. Dwarakanath, N. Uday Shankar and K. R. Subramanian although many others whose names are too numerous to list here have significantly contributed to the decameter wave radio telescope project. I would like to thank all of them for many stimulating discussions and for allowing me to quote their work.

### References

- Deshpande, A. A.: 1992, *J. Astron. Astrophys.* **13**, 167.  
 Deshpande, A. A. and Radhakrishnan, V.: 1992, *J. Astron. Astrophys.* **13**, 151.

- Deshpande, A. A. and Sastry, Ch. V.: 1986, *Astron. Astrophys.* **160**, 129.
- Deshpande, A. A., Sastry, Ch. V., and Radhakrishnan, V.: 1984a, in W. C. Erickson and H. V. Cane (eds.), *Proc. Workshop on Low Frequency Radio Astronomy held at NRAO, Green Bank, U.S.A.*
- Deshpande, A. A., Shevgaonkar, R. K., and Sastry, Ch. V.: 1984b, *Astrophys. Space Sci.* **102**, 21.
- Deshpande, A. A., Shevgaonkar, R. K., and Sastry, Ch. V.: 1989, *J. IETE* **35**, 342.
- Dwarakanath, K. S.: 1991, *J. Astron. Astrophys.* **12**, 199.
- Dwarakanath, K. S. and Uday Shankar, N.: 1990, *J. Astron. Astrophys.* **11**, 323.
- Dwarakanath, K. S., Shevgaonkar, R. K., and Sastry, Ch. V.: 1982, *J. Astron. Astrophys.* **3**, 207.
- Sastry, Ch. V.: 1972, *Astrophys. Letters* **1**, 47.
- Sastry, Ch. V.: 1973, *Solar Phys.* **28**, 197.
- Sastry, Ch. V.: 1989, *Indian J. Pure Appl. Phys.* **27**, 331.
- Sastry, Ch. V.: 1994, *Solar Phys.* **150**, 285.
- Sastry, Ch. V. and Shevgaonkar, R. K.: 1983, *J. Astron. Astrophys.* **4**, 47.
- Sastry, Ch. V., Dwarakanath, K. S., Shevgaonkar, R. K., and Krishan, V.: 1981a, *Solar Phys.* **73**, 363.
- Sastry, Ch. V., Dwarakanath, K. S., and Shevgaonkar, R.K.: 1981b, *J. Astron. Astrophys.* **2**, 339.
- Sastry, Ch. V., Shevgaonkar, R. K., and Ramanuja, M. N.: 1983, *Solar Phys.* **87**, 391.
- Subramanian, K.R., Nanje Gowda, C., Abdul Hameed, A. T. H., and Sastry, Ch. V.: 1986, *Bull. Astron. Soc. India* **14**, 236
- Subramanian, K.R., Sundararajan, M.S., and Sastry, Ch. V.: 1994, *Proc. of the IAU Sixth Asian Pacific Regional Meeting on Astronomy, J. Astron. Astrophys.*, in press.
- Uday Shankar, N. and Ravi Shankar, T. S.: 1990, *J. Astron. Astrophys.* **11**, 297.